

Structural control of the São Francisco River Delta from the aeromagnetic data, Brazil.

1 ABSTRACT

2
3
4
5
6
7
8
9
10
11
12
13
14
15
16
17
18
19
20
21
22
23
24
25
26
27
28
29
30

The São Francisco River delta is a Quaternary sandy plain built on a structural low of the Sergipe-Alagoas Basin, known as the São Francisco Low. The inner limit of the São Francisco River delta is defined by rectilinear cliffs between the delta plain and the Barreiras Formation, which coincide with important faults delimiting the São Francisco Low. Moreover, on the continental shelf, the deltaic clinoform developed over a topographic low limited by rectilinear scarps that present compatible orientation with the Sergipe-Alagoas structural framework. Thus, based on a theoretical background that indicates the existence of structural control over the formation of delta systems in general, and previous knowledge of this area, it is possible that the Sergipe-Alagoas Basin structure has influenced the delta. This relationship can be inferred using adequate methodology. Magnetometric data was integrated in the present study with the geological information on the area. The main objective was to evaluate the existing structural controls over the formation of the São Francisco delta and neighboring areas. The first stage of the present study consisted of a thorough bibliographic review and the search for pre-existing geophysical data in the region.

Keywords: Delta; San Francisco; Aeromagnetic Data; Edge Detection.

1. INTRODUCTION

Deltas are defined as a shoreline protuberance caused by the insertion of the fluvial system into a lower energy environment, in a context where the sedimentary supply is greater than the capacity of the basin to distribute ([2], [3]). Deltaic environments are of great importance since these areas offer various facilities for the populations that settle in them. As an example are the fertile land regions for agriculture, the proximity to river courses and the coastal zone [11].

Nowadays, many studies are carried out in deltas that target the oil and gas industry, but studies that are concerned with the environmental aspects of these regions have also been developed [11]. The significant increase in the environmental impacts caused by the increase of the population in these areas has generated an increasing concern with them, very susceptible to problems such as coastal erosion, subsidence, floods and salt intrusion [19].

There are several factors that are widely found in the literature, which are identified as those responsible for delta sedimentation: climate, river discharge, tidal amplitudes, wave energy, relative sea level variation, wind patterns ([4], [7], [8], [9]). Another important factor in the deltaic sedimentation is the tectonics of the area, which although little approached as one of the determining factors in this process presents evidences of its control in deltas around the world.

Some works present in the literature analyze the tectonics as the main controlling agent in the formation of the deltas. **Research by GOODBRED *et al.* [12]** on the Ganges-Brahmaputra delta, emphasized the influence of Himalayan tectonics on the sedimentation

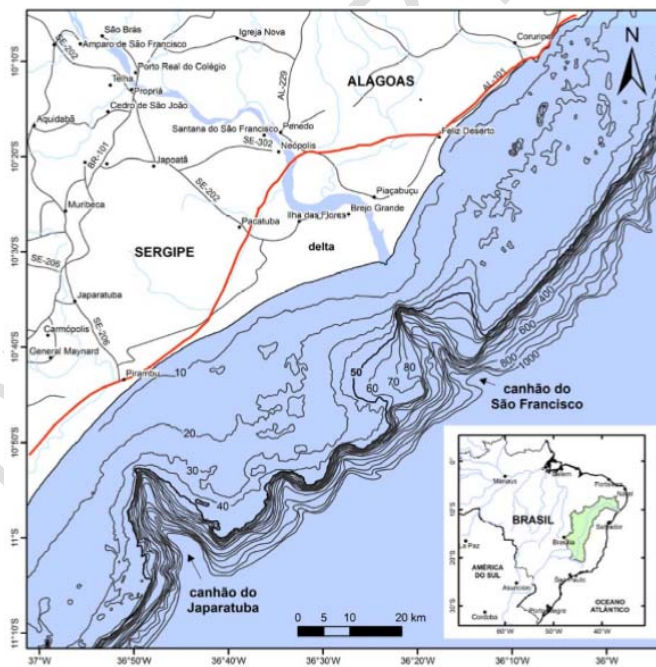
31 rates, magnitude and characteristics of the sedimentary deposits on the delta banks.
32 **CARMINATI, MARTINELLI and SEVERI [5]** researched about the Pos Delta and the
33 influence of glacial cycles and tectonic processes on the natural subsidence of this delta.

34 **ARMSTRONG et al. [1]** developed a study that shows the influence of the presence
35 of reactivated growth faults in the Mississippi Delta, and **STANLEY [20]** developed a study
36 that attempted to understand subsidence processes in the Nile Delta, where he concluded
37 that subsidence rates were accelerated due to the neotectonic present in the region. Finally,
38 **LIMA et al. [15]** researched the São Francisco Delta that focused on the study of the
39 reactivation of faults in the Quaternary as the main controlling agent of sediment deposition
40 and morphology of this delta.

41 The São Francisco River Delta (DSF) is a sandy, quaternary-level plain (Figure 1)
42 built on a low basement of the Sergipe-Alagoas basin, known as Baixo do São Francisco
43 [19]. Knowledge about DSF is basically restricted to its superficial outcrop portion.
44 **GUIMARÃES [11]** was the first to provide subsurface information of the area, which allowed
45 to advance in the knowledge of the depositional architecture of this system. A preliminary
46 analysis of published works and existing data suggest some kind of tectonic control in the
47 development of DSF.

48 The Sergipe-Alagoas Basin, located in the states of Sergipe and Alagoas, is
49 distributed both on land and in the submerged region, extending towards the sea beyond the
50 2,000 m isobath, in a total area of approximately 34,600 km², being 12,000 km² in the
51 emergent portion. This basin is limited by the parallels 9°S and 11°30'S and by the meridians
52 34° 30'W and 37° 30'W.

53
54



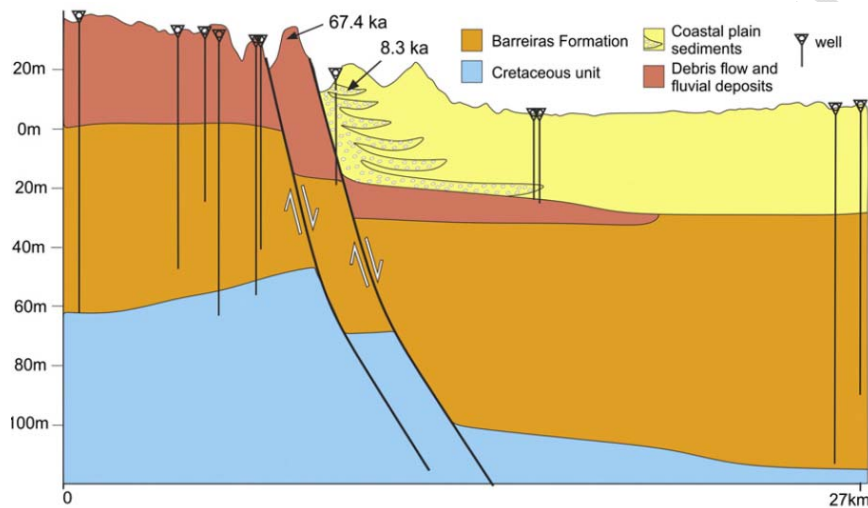
55

Figure 1: Location map of the study area. Source: [11].

56
57
58
59
60
61

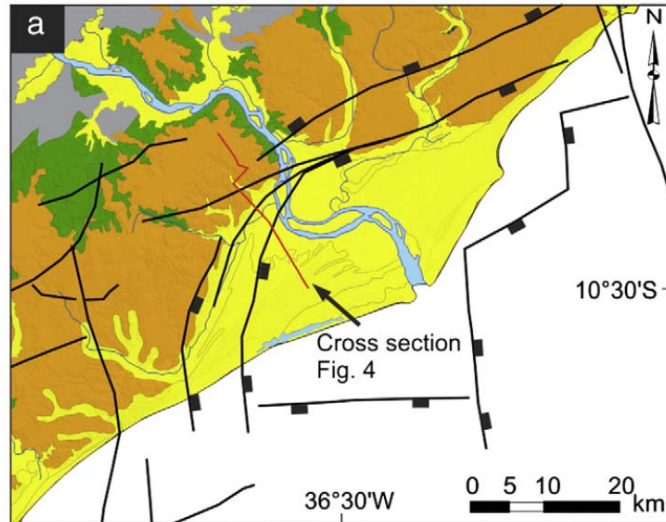
In a more recent work, **LIMA et al. [15]** researched the DSF that had as main focus the process of reactivation of faults in the Quaternary, considered by the author as the main controlling agent of sediment deposition and delta morphology. This control would occur from the generation of new space for sediment accommodation, through the reactivation of faults. This work using well data, optical and radiocarbon dating and seismic data proposed

62 the existence. From three main stratigraphic units (Figure2): 1) Barreiras Formation deposits
 63 (fb) dated from the Miocene; 2) fluvial deposits and flow of debris (dff) dated to the Late
 64 Quaternary; 3) inter bedded braided stream (bsb) deposits also dated from the Late
 65 Quaternary. Data from pre-existing seismic surveys in the region show that the internal
 66 boundary of the DSF coincides with the N-S and NE-SW direction of Cretaceous faults.
 67 These faults form several cliffs and most of these are at the base of the uncontaminated
 68 sedimentary rocks of the fb and the dff unit.
 69
 70
 71
 72
 73
 74



75
 76 **Figure 2:** Main stratigraphic units found in the area: 1) Barreiras Formation deposits (fb); 2)
 77 Fluid deposits and flow of debris (dff); 3) Braided stream (bsb) deposits. (Source: [15]).
 78

79
 80
 81 The author concludes that at least two major faults were reactivated during the
 82 Miocene. In Figure 3 it is possible to verify the Cretaceous faults with a parallel orientation to
 83 the internal boundary of the delta plain plunging toward the basin. Figure 2 shows an
 84 increase in the thickness of the Barreiras Formation, crossing these faults, suggesting a
 85 sediment deposition contemporary to the failure processes, with reactivation of these faults
 86 during the Miocene. LIMA *et al.* [15] also presented evidence of other reactivations during
 87 the Pleistocene-Holocene that affected or created additional accommodation space for the
 88 deposition of the other units. The Figure 3 shows the geological map evidencing the present
 89 failures in the region and the limits of the DSF.
 90
 91
 92



93
94
95
96

Figure 3: Simplified geological map evidencing the present failures in the region and the limits of the DSF. The cross section in red represents the section shown in Figure 2 (Source: [15]).

The present work consists in the use of the integrated magnetometry method to the geological data about the study area, having as main objective the evaluation of the structural controls in the formation and evolution of the DSF. While potential methods provide us with more general information on these controls, the seismic method is able to provide information in higher definition of subsurface geological features.

It consists of the interpretation of maps generated from the aeromagnetic data, such as the Map of the Tilt Angle of the Horizontal Total Gradient (TAHG) that allows us to visualize in subsurface the presence of magnetic bodies and their contacts, besides the generation of a quantitative solution in depth. Magnetic maps are frequently used to delineate geologic contacts and border of geological formation. These maps have signals with various amplitudes that originate from different geometric sources, situated at different depths and with different magnetic properties.

97
98

2. MAGNETOMETRIC METHOD

99
100
101
102
103
104
105
106
107

The development of the databases involved merging numerous surveys with aeromagnetic data with highly variable specifications and quality [6]. The integrated and corrected anomaly maps were processed and interpreted. Knowing the magnetic anomaly it was possible to estimate the depth top and bottom, magnetic lineaments, faults, blocks, the lateral extension, the width of the sources. From these results, we can produce a geological interpreting and understanding the tectonic environment. For regional exploration, magnetic measurements were important for example, continental boundaries of terrain were commonly recognized by magnetic contrast in all contact. Such regional interpretations required continental scale for magnetic databases.

108
109
110
111
112
113

The magnetometry data used in this work belong to the database of CPRM (Mineral Resources Research Company) and was assigned to this study by the Laboratory of Nuclear Physics and Environment of the Federal University of Bahia. The data includes two aeromagnetic surveys carried out in the region encompassing the Deltaic Plain of the São Francisco River belonging to the projects 1102_ESTADO_DE_SERGIPE and 11_04_PAULO_AFONSO_TEOTÔNIO_VILELA (Figure 4).

114

115 The aeromagnetic projects have a spacing of flight lines of 500 m oriented in the N-
116 S direction, with flight height of 100 m, the interval between measurements of the
117 magnetometer of 0.1 s and the spectrometer 1.0 s. The survey was carried out in two
118 different blocks with different flight and tie-line directions, and data acquisition was
119 performed perpendicular to the main structures of the surveyed area [6]. The magnetic data
120 of the study area generated from the pre-processed data, using different combinations of
121 parameters, the cell size of 1/4 of the flight line. Grids of the magnetic anomaly were
122 generated and then a database of each grid generated around the Sergipe-Alagoas Basin
123 defining the study area. The magnetic system used was an optically pumped (cesium vapor)
124 magnetometer that was installed in a stinger extension behind the tail of the aircraft. The
125 output from the magnetometer was sampled at 0.1 s to a resolution of 0.001 nT with a noise
126 envelope less than 0.01 nT.

127

128 In the next processing step, the data were interpolated to a regular grid, using
129 algorithms that maintain data fidelity at the original measurement locations. This step was
130 followed by correction of spurious effects caused by the leveling of the original grids. The
131 fourth-order difference technique was used to track anomalous spikes in the magnetic data
132 and to condition sampling along the flight lines based on the spatial Nyquist frequency. This
133 was performed on the selected interpolated grid, which contained square cells 125 x 125 m.
134 The algorithm was based on linear interpolation along the direction of the flight lines, and on
135 the Akima spline perpendicular to the flight lines. Microleveling and decorrugation techniques
136 were applied to the data. This procedure resulted in several geophysical data products,
137 including thematic maps of both individual variables and composite variables, for use in
138 geologic analysis and interpretation.

139 Usual linear transformations were applied to the magnetic data to process changes
140 in the amplitude and/or phase related to the set of the data [14]. These transformations are
141 carried out by multiplying the Fourier transform in the data set in the frequency domain. The
142 inverse Fourier transform returns to the space domain and gives the current field to the
143 upper level. This is equivalent to convolving the field in the space domain by an operator (or
144 filter). All transformations of the magnetic field work on this path. For the magnetic data
145 processing, a regional-residual separation process was required to obtain the subject of
146 interest of this study. To do so, an upward continuation was performed, where the estimated
147 depth value used in this process was obtained through radially average power spectrum
148 analysis of the magnetic data.

149 The aeromagnetic data assigned to this work was in its raw state and its treatment
150 followed a characteristic route: application of the equation reduction filter of the anomalous
151 magnetic field data, power spectrum analysis and regional-residual separation from
152 upwards. The calculation of the field at higher levels is called continuation upwards and
153 proposes the removal of high frequency anomalies relative to low frequency anomalies.

154 After the Total Magnetic Field (TMF) data was reduced to the Equator, two
155 ascending continuations were applied, one for 100 m and the other for 1000 m, which were
156 defined from the power spectral study of the magnetic signal. The first allowed the removal
157 of low frequencies that are characterized by superficial noises and the second allowed the
158 elimination of deeper frequencies. The grids generated in both processes were subtracted
159 (regional / residual separation) so that the resulting magnetic information is related only to
160 geological features that extend up to approximately 1000 m depth. The gross TMF and TMF
161 maps after the RE and CA steps are shown in [Figures 4a and 4b](#).

162

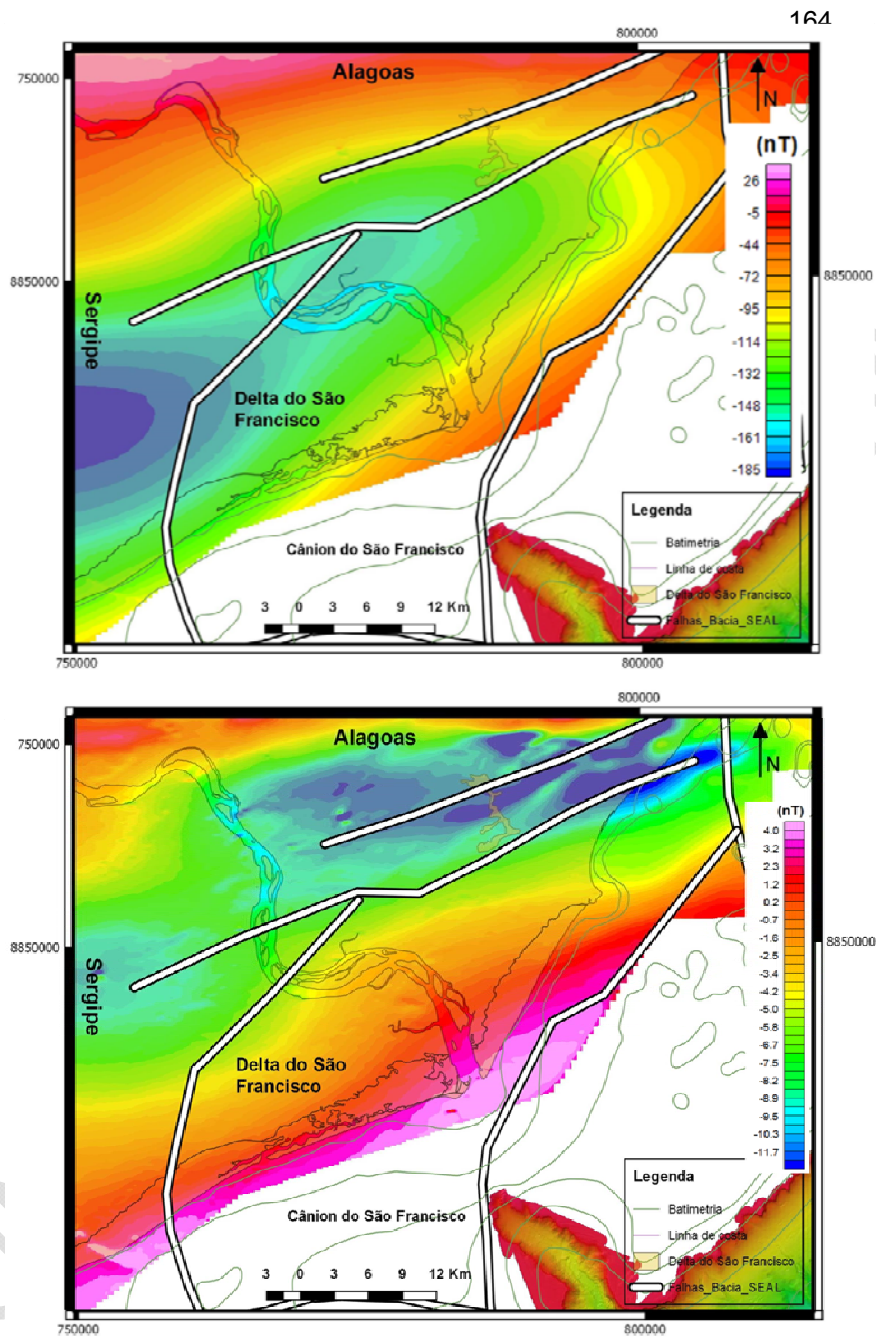
208
209

Figure 4: A) TMF map; B) and TMF map reduced to the equator and continued upward with regional / residual subtraction.

210 FERREIRA *et al.* [10] presented an edge detection method that is based on the
211 enhancement of the THG of magnetic anomalies using the Tilt Angle. It is referred to as the
212 tilt angle of the horizontal gradient (TAHG). In this study, efficiency of the TAHG is
213 considered for magnetic data set. The TAHG transform range is from $-\pi/2$ to $+\pi/2$ (Figure 5).

214 From this, some enhancement methods were used that gave rise to the Analytical
215 Signal Anomaly (ASA), Total Horizontal Gradient (THG), and Total Horizontal Gradient
216 Analytical Signal Slope (TAHG) maps. Both enhancements are best described below.

217
218 1) Amplitude of the Signal Analytic (ASA): Asymmetric function in bell format that
219 aims to delimit magnetic bodies and to centralize them above their sources [13]. The ASA
220 map represents magnetic anomalies free of noise and the influence of deep sources.

221 2) Total Horizontal Gradient (THG): A highlight technique that allows
222 distinguishing the lateral boundaries of anomalous sources through abrupt changes in the
223 physical properties of lithology. In the THG map the maximum values of the anomalies are
224 located on the edge of the anomalous source.

225 3) Total Total Horizontal Gradient Analytical Signal Slope (TAHG): TAHG
226 enhances GHT through subsequent application of analytic signal slope [10]. The method
227 centralizes the maximum amplitude at the edges of the magnetic sources and different from
228 the GHT is not related to the depth of the same.

229 In addition to the corrections and the generation of the enhancement maps that
230 characterize a qualitative data analysis, quantitative solutions were also generated from the
231 SPI method. The SPI method calculates three attributes of the Complex Analytical Signal,
232 amplitude, phase and local frequencies, which allow us to calculate the Local Probability
233 Depth, Diving and Contrast parameters of the magnetic sources ([16], [21]).

234

235

236 3. RESULTS AND DISCUSSION

237

238 The methods were used that gave rise to the Analytical Signal Anomaly (ASA), Total
239 Horizontal Gradient (THG), and Total Horizontal Gradient Analytical Signal Slope (TAHG)
240 maps. The Figure 5 shows respectively the ASA, THG, TAHG and SPI solution maps.

241

242 Then analysis of all products generated with the magnetic data was performed and
243 the maps chosen for joint interpretation were: TMF reduced to the equator and continued
244 upwards, TAHG and map with SPI in-depth solution. In the TMF map (Figure 6) it was
245 possible to individualize the main magnetic regions of the study area:

246

- 247 1) Region of very low magnetic amplitudes; F.
- 248 2) Region of low magnetic amplitudes;
- 249 3) Region of intermediate magnetic amplitudes; D.
- 250 4) Region of high magnetic amplitudes: C.
- 251 5) Regions of very high magnetic amplitudes: A, B.

252

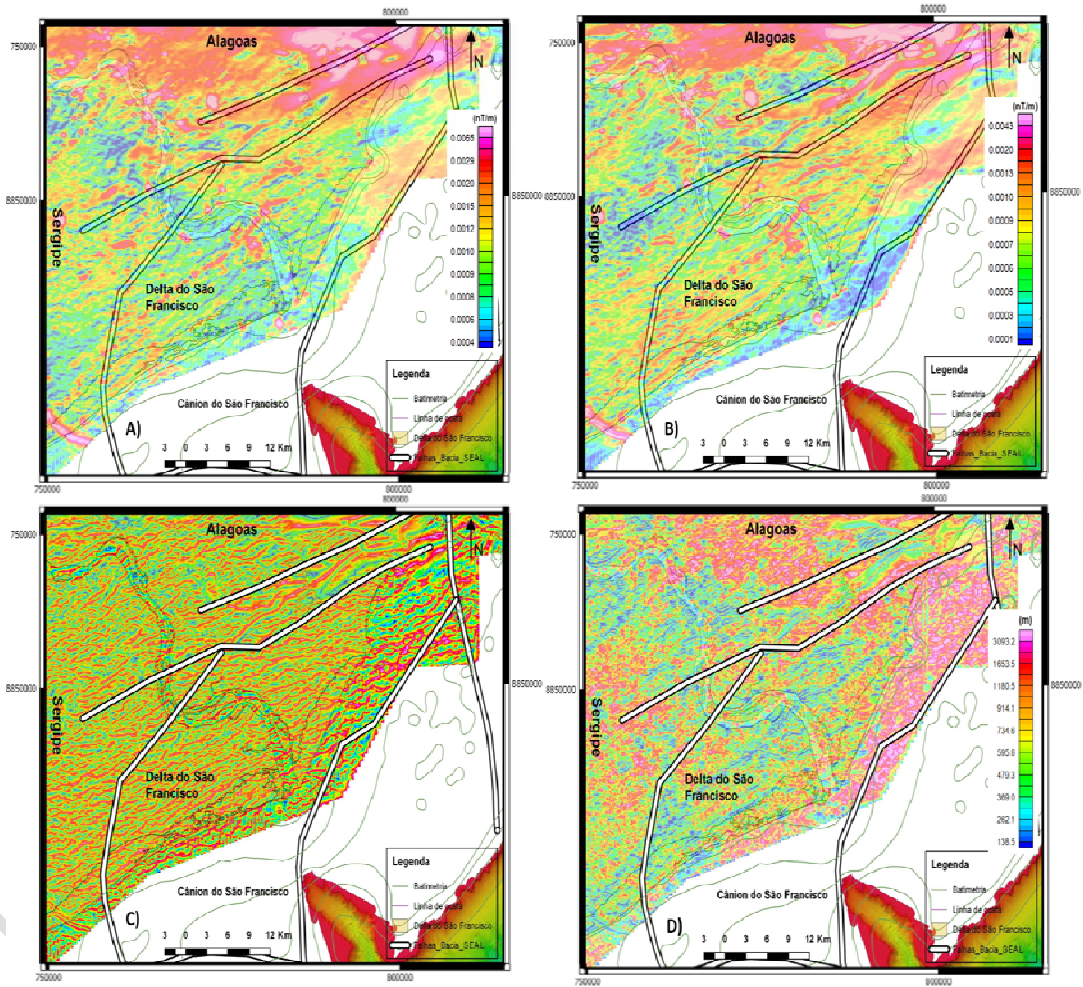
253 With respect to the TMF map and its magnetic regions, it is possible to observe that
254 there is a tendency in the increase of the magnetic field when approaching the coastline,
255 expected factor since the sea behaves like a great conductor and influences positively in the
256 values from Camp. The regions E and F characterized as zones of low and very low
257 magnetic field, respectively, may be associated to existing depocenters within the Sergipe-
258 Alagoas basin, since a large column of sedimentary material would increase the distance to
259 the basement of the basin and present smaller values of magnetic field.

260 The TAHG map (Figure 7) was interpreted and the main magnetic lineaments of the
261 study area were duly marked. The joint analysis of this interpretation with the map of the SPI
262 solution (Figure 8) allowed us to individualize the bodies and their respective depths.

263 Another important feature observed in the map interpreted TAHG is the preferred direction of
 264 the magnetic lineaments. These, in turn, have preferential directions NE-SW and E-W, in
 265 addition to some NW-SE perpendicular structures. These directions coincide with the tracing
 266 of the main flaws that constitute the structural framework of the Sergipe-Alagoas basin.

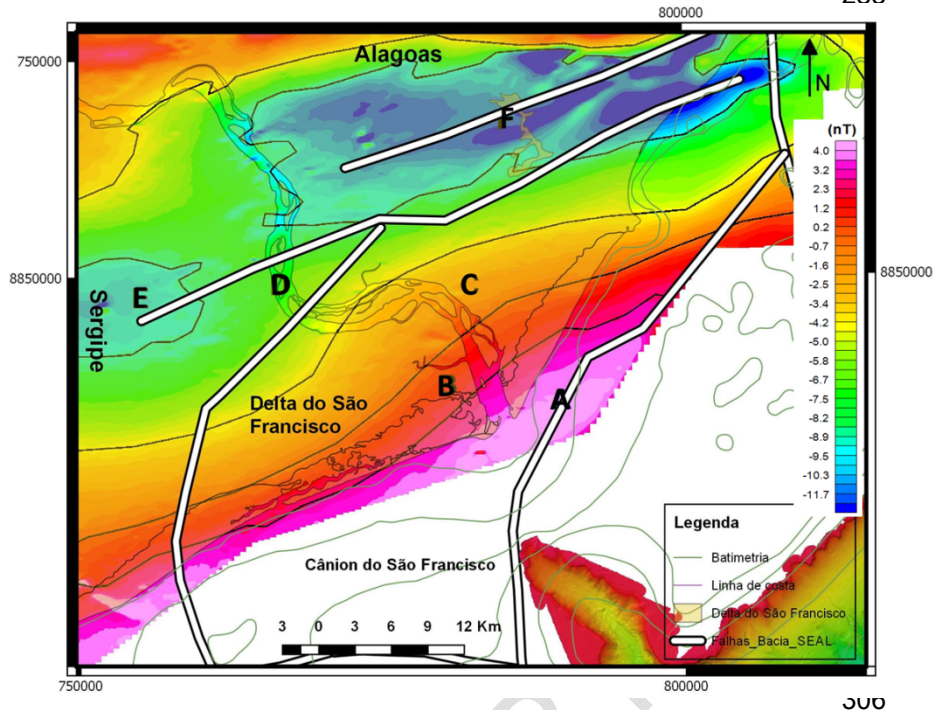
267 Based on depth information obtained in the SPI solution map, it is possible to verify
 268 that the interpreted magnetic lineaments, which in turn may correspond to contact regions or
 269 faults, on the TAHG map are at a maximum depth of about 1200 m, which leads us to
 270 suggest that the faults in the structural framework of the SE-AL basin, which are deeper,
 271 have an extension to shallower regions.

272
 273



274
 275
 276
 277
 278
 279
 280
 281
 282

Figure 5: A) ASA map; B) Map of THG; C) TAHG Map; D) Map of SPI.



307 **Figure 6:** Map of TMF reduced to the equator and continued upward with its main
 308 individualized magnetic regions.

309 On the magnetic information obtained in this work, we have the maps of TAHG
 310 (Figure 7) and the SPI depth solution (Figure 8) superimposed on the study area. It was
 311 previously highlighted the existence of a preferential direction of the magnetic lineaments
 312 found in the region, they are parallel or subparallel to important flaws that delimit the
 313 structural framework of the SE-AL basin. Note that the magnetic lineages on the DSF are
 314 very shallow when observing the depth values of the region on the SPI map, which
 315 suggests that they may be the expression of coastal strands in the delta plain.

316 Another important point to note is the marking of the magnetic lines that delimit the San
 317 Francisco low on the TAHG map (area 1 and 2 on the map). The blue lineages on the map
 318 (Figures 7 and 8) were interpreted as the region of rectilinear cliffs belonging to the
 319 Barreiras Formation and are the internal boundaries of the deltaic plain with formation. Note
 320 that these cliffs accompany the tracing of lineages belonging to the SE-AL basin, which,
 321 according to Ponte [17], shows a direct influence of the basin structuring on the formation of
 322 the DSF. Another important aspect to be noticed is the regions A and B, of the SPI solution
 323 map, which present higher values of depth and continue to reinforce the idea of the
 324 presence of depocenters of the basin.

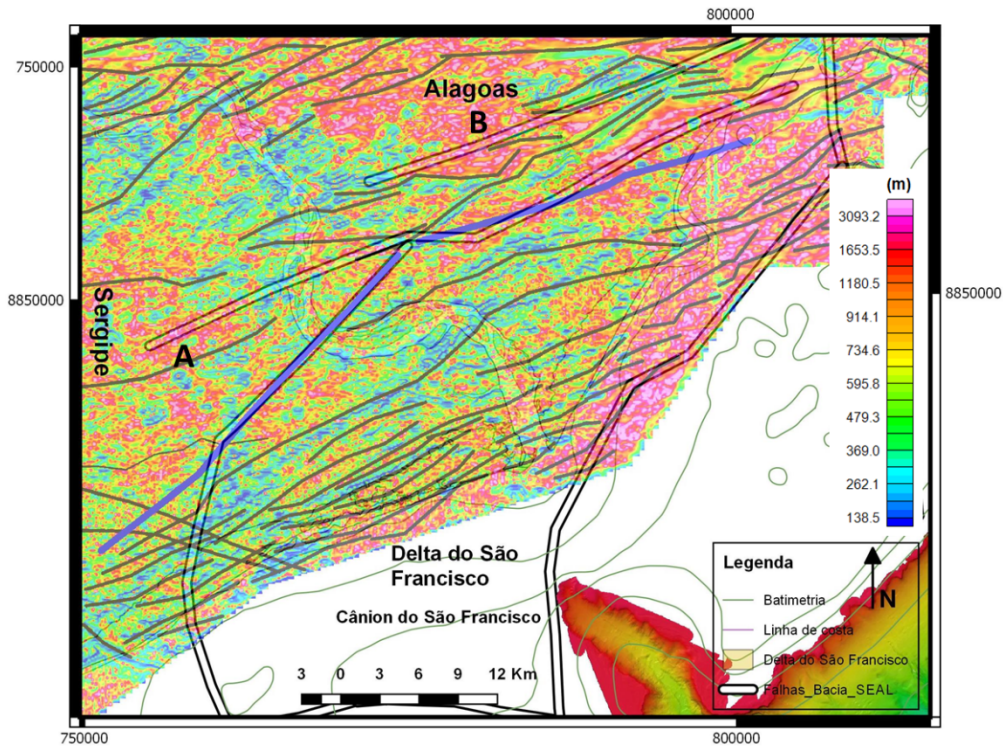
325

326 It was possible to identify, from the joint analysis of all the information generated
 327 and pre-existing, the presence of a set of faults that directly affect the sedimentation in the
 328 region. However, previous knowledge of the geology of the area leads us to believe that the
 329 observed faults would not be related to a possible reactivation of tectonic character, but to
 330 processes that involve material overload and consequent gravitational collapse of the region
 331 being studied.

332

333

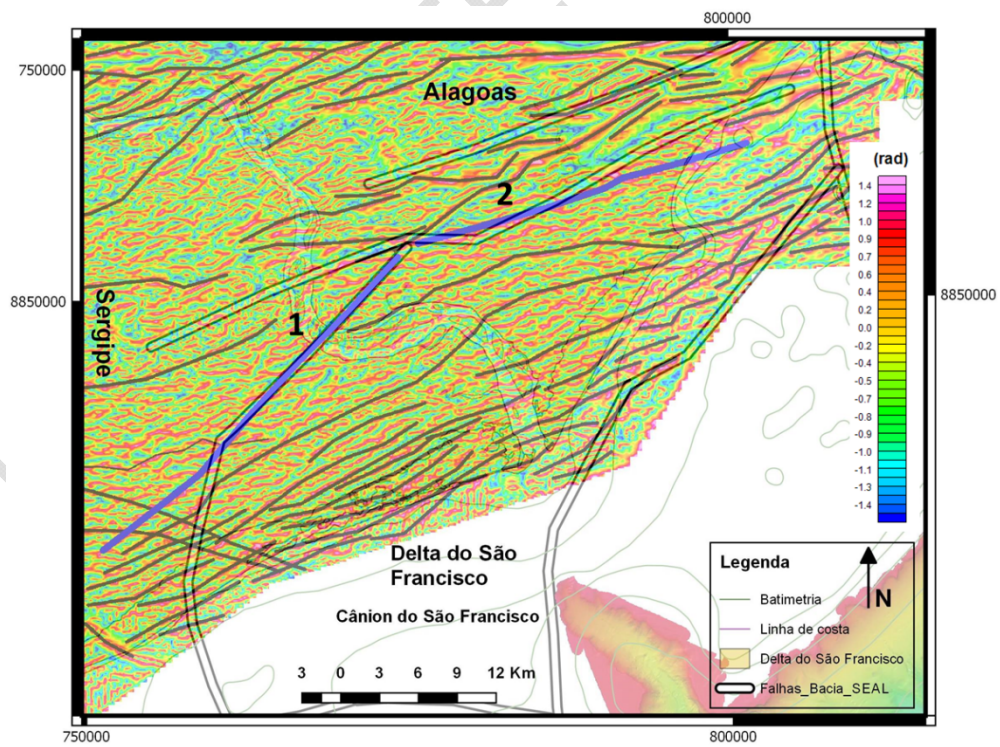
334



Figura

359 **re 7:** Interpreted TAHG map. The lines marked in black represent the marked magnetic
 360 lineaments and the blue lines the deltaic plain with the Barreiras Formation.
 361
 362

363
 364
 365
 366
 367
 368
 369
 370
 371
 372
 373
 374
 375
 376
 377
 378
 379
 380
 381
 382
 383
 384
 385
 386



387 **Figure 8:** SPI solution map. The lines marked in black represent the marked magnetic
388 lineaments and the blue lines the deltaic plain with the Barreiras Formation.
389

390 **4. CONCLUSION**

391 The present work presents the results of a joint analysis of magnetic data and previous
392 geological and geophysical information of the area comprising the DSF and its environment.
393 There has been an attempt to understand the structural controls that affect the origin and
394 evolution of the delta, whether these controls are associated with a new tectonic present in
395 the region and whether the structuring of the SE-AL basin also exerts some influence. The
396 treatment and interpretation of the aeromagnetic data provided us with a design of the
397 magnetic framework of the region, where it was possible to show the main lineaments in the
398 area. It was also possible through the magnetic die to mark the inner boundary of the delta
399 plain. Thus, the greatest contribution of this method was to the information on the geological
400 aspect of the area, which together with the Bouguer anomaly map of the region provided us
401 with more precision, the expression of coastal strands presents in the delta sedimentation,
402 the marking of possible depocenters of the basin and the limits of the delta. It was not
403 possible to identify in this work the presence of a more recent and active tectonic in the
404 region, so the origin of the failures that exert a structural control in the area can be
405 associated with mass gravitational collapses driven by the overload of material deposited in
406 the region.

407

408

409 **ACKNOWLEDGEMENTS**

410

411 We are grateful to the CPRM (Brazilian Geology Program) for the Aerogeophysical
412 Projects for granting the data used in this work.
413

414

415

416

417 **REFERENCES**

418

419 1. ARMSTRONG C., MOHRIG D., HESS T., GEORGE T., STRAUB K. M., 2014. Influence
420 of growth faults on coastal fluvial systems: Examples from the late Miocene to Recent
421 Mississippi River Delta, *Sedimentary Geology* 301, 120–132.

422

423 2. BITTENCOURT, A.C.S.P.; DOMINGUEZ, J.M.L.; FONTES, L.C.S.; SOUSA, D.L.; SILVA,
424 I.R.; SILVA, F.R., 2007. Wave refraction, river damming, and episodes of severe shoreline
425 erosion: the São Francisco river mouth, northeastern Brazil. *Journal of Coastal Research*. 23
426 (4), p. 930-938.

427

428 3. BHATTACHARYA, J.P.; GIOSAN, L., 2003. Wave-influenced deltas: geomorphological
429 implications for facies reconstruction. *Sedimentology*. 50, p.187-210.

430

431 4. BHATTACHARYA, J. P.; WALKER, R. G., 1992. Deltas. In: WALKER, R. G.; JAMES, N.
432 P. (eds.): *Facies Models - Response to sea level change*. Toronto. Geological Association of
433 Canada, p. 157-178.

434

435 5. CARMINATI, E., MARTINELLI, G., and SEVERI, P., 2003, Influence of glacial cycles and
436 tectonics on natural subsidence in the Po Plain (Northern Italy): Insights from 14C ages:
437 *Geochemistry, Geophysics, Geosystems*, v. 4, p. 1082.

- 438 6. CPRM, 2008. Projeto Aerogeofísico Borda Leste do Planalto da Borborema, CPRM
439 (Programa Geologia do Brasil).
440
- 441 7. DOMINGUEZ, J.M.L., 1990. Delta dominados por ondas: críticas às idéias atuais com
442 referência particular ao modelo de Coleman & Wright. *Revista Brasileira de Geociências*, 20
443 (1-4), p. 352-361.
444
- 445 8. DOMINGUEZ, J.M.L., 1996. The São Francisco strand plain: a paradigm for wave-
446 dominated deltas. *Geological Society Special Publication* 117: 217-231.
447
- 448 9. DOMINGUEZ, J.M.L.; BITTENCOURT, A.C.S.P; MARTIN, L., 1981. O papel da deriva
449 litorânea de sedimentos arenosos na construção das planícies costeiras associadas às
450 desembocaduras dos rios São Francisco (SE-AL), Jequitinhonha (BA), Doce (ES) e Paraíba
451 do Sul (RJ). *Revista Brasileira de Geociências*. 13(2). 1983. p. 98-105.
452
- 453 10. FERREIRA, F. J. F.; de SOUZA, J.; de BARROS, A.; BONGIOLO, S.; de CASTRO, L. G.
454 e ROMEIRO, M. A. T., 2010. Realce do gradiente horizontal total de anomalias magnéticas
455 usando a inclinação do sinal analítico. parte I-aplicação a dados sintéticos, In:IV Simpósio
456 Brasileiro de Geofísica.
457
- 458 11. GUIMARÃES, J.K., 2010. Evolução do delta do rio São Francisco – estratigrafia do
459 Quaternário e relações morfodinâmicas. Tese (Doutorado em Geologia) - Universidade
460 Federal da Bahia. Instituto de Geociências. Orientador: José Maria Landim Dominguez.
461 2010. 127 p.
462
- 463 12. GOODBRED, S.L., Jr., KUEHL, S.A., STECKLER, M.S., and SARKER, M.H., 2003.
464 Controls on facies distribution and stratigraphic preservation in the Ganges-Brahmaputra
465 delta sequence: *Sedimentary Geology*, v. 155, p. 301–316.
466
- 467 13. GUNN, P.J., 1997. Quantitative methods for interpreting aeromagnetic data: a subjective
468 review. *Journal of Australian Geology & Geophysics*, v.17, n.2, p. 105-113.
469
- 470 14. Hood, P.J. and Teskey, D.J., 1989. Aeromagnetic gradiometer program of the Geological
471 Survey of Canada. *Geophysics*, 54 (8), 1012–1022.
472
- 473 15. LIMA, C.U., BEZERRA, H.R., NOGUEIRA, C. C., RUBSON, P., SOUZA, O.L., 2014,
474 Quaternary fault control on the coastal sedimentation and morphology of the São Francisco
475 coastal plain, Brazil. *Tectonophysics*, 633, 98-114.
476
- 477 16. NABIGHIAN, M. N., 1972. The analytic signal of two-dimensional magnetic bodies with
478 polygonal cross-section: Its properties and use for automated anomaly interpretation,
479 *Geophysics*, 37(1):507-517.
480
- 481 17. PONTE, F.C. (1969), **Estudo Morfo-Estrutural da Bacia Alagoas-Sergipe – Bol. Tec.**
482 **Petrobras 12 (4): 439, 474.**
- 483
- 484 18. SÁNCHEZ-ARCILLA, A.; JIMENÉZ, J.A.; VALDEMORO, H.I., 1998. The Ebro delta:
485 morphodynamics and vulnerability. *Journal of Coastal Research* 14 (3): 754–772.
486
- 487 19. SOUZA-LIMA, W. Litoestratigrafia e evolução tectono-sedimentar da bacia de Sergipe-
488 Alagoas, introdução. *Fundação Paleontológica Phoenix*. Aracaju. Ano 8. n. 89. 2006.
489

- 490 20. STANLEY D.J., 1988, Subsidence in the northeastern Nile delta: Rapid rates, possible
491 causes, and consequences: Science, v. 240, p. 497–500.
492
493 21. THURSTON, J. B. e Smith, R. S., 1997. Automatic conversion of magnetic data to
494 depth, dip, and susceptibility contrast using the SPI (tm) method, Geophysics, 62(3):807.

UNDER PEER REVIEW